

Inferring fine-grained migration patterns across the United States

Gabriel Agostini¹, Rachel Young², Maria Fitzpatrick³, Nikhil Garg¹,
Emma Pierson²

¹Cornell Tech, New York City, NY, United States.

²University of California, Berkeley, Berkeley, CA, United States.

³Cornell University, Ithaca, NY, United States.

Abstract

Fine-grained migration data illuminate important demographic, environmental, and health phenomena. However, migration datasets within the United States remain lacking: publicly available Census data are neither spatially nor temporally granular, and proprietary data have higher resolution but demographic and other biases. To address these limitations, we develop a scalable iterative-proportional-fitting based method which reconciles high-resolution but biased proprietary data with low-resolution but more reliable Census data. We apply this method to produce MIGRATE, a dataset of annual migration matrices from 2010 - 2019 which captures flows between 47.4 billion pairs of Census Block Groups — about four thousand times more granular than publicly available data. These estimates are highly correlated with external ground-truth datasets, and improve accuracy and reduce bias relative to raw proprietary data. We publicly release MIGRATE estimates and provide a case study illustrating how they reveal granular patterns of migration in response to California wildfires.

1 Introduction

Fine-grained migration data, which record the number of people relocating from one geographic area to another, are essential for understanding a range of social, environmental, and health phenomena. Migration patterns illuminate responses to environmental disasters and climate change [1–3]; responses to economic stresses and opportunities [4–6]; patterns of social change [7]; effects of the COVID-19 pandemic [8]; and political polarization [9].

But migration data within the United States have serious limitations. The most fine-grained freely available datasets track migration at the county level. While widely used, these datasets lack sufficient spatial resolution to study a number of phenomena where previous research has revealed important variation at the sub-county level. For example, research on flood-risk-induced migration uses models at the much more granular Census block level [10], arguing that this spatial granularity is necessary due to the highly localized nature of flood risk [11]. Research on neighborhoods which are vulnerable to climate-induced eviction or displacement similarly models risk at a sub-county (Census tract) level [12]. Movers within the same county have accounted for more than half of migratory flows in the United States in all years from 2006 to 2019 [13]. Publicly available, county-level migration datasets render these patterns entirely invisible.

Proprietary migration datasets offer greater granularity. Data aggregators like Infutor [14] combine many data sources — including voter files, property deeds, credit files, and phone books [15] — to attempt to infer address histories for individual-level movers. Such datasets have been widely used because they are extremely temporally and spatially fine-grained [4, 16–19]. Previous work

also suggests these data do contain valuable signal which correlates with external datasets, as validated by cross-referencing the data with hurricanes or public housing foreclosures [16], and with marginal population counts in the region of interest [15]. However, these proprietary datasets have three major disadvantages. First, they are not publicly available, limiting their utility to researchers. Second, they require extensive computational pipelines, and substantial computational resources, to clean and map to standardized geographical areas to facilitate subsequent analysis. Third, and most fundamentally, they combine multiple imperfect data sources using proprietary algorithms, and thus contain noise and biases. For example, Infutor and other consumer record datasets have been shown to overrepresent higher-income and majority-group populations in some settings [20].

To address these limitations of existing migration data, we create and release **MIGRATE** (**M**igration **I**nference for **GR**Anular **T**rend **E**stimation): fine-grained migration estimates which combine the strengths of both aforementioned types of data by harmonizing biased but fine-grained proprietary data with reliable but coarse Census data. To produce our estimates, we develop a method based on iterative proportional fitting (IPF), an algorithm which repeatedly scales a noisy matrix to reconcile it with constraints [21], to reconcile the raw Infutor migration matrix with the more reliable Census constraints. We accommodate uncertainty in address mapping and incorporate data on births, deaths, and immigration. The output of our method is a set of yearly inferred migration matrices at the Census block group (CBG) level from 2010-2019 covering the 50 states and the District of Columbia. Our matrices capture migration flows between 47.4 billion pairs of CBGs, making **MIGRATE** approximately 4,600 times more granular than the county-county flows which are currently available on the 5-year level, and 18 million times more granular than the state-state flows which are currently available on the 1-year level.

We comprehensively validate **MIGRATE** by comparing it to external data sources. We show that our estimates correlate well with fine-grained Census and ACS data on population counts and migration flows. We show that **MIGRATE** improves accuracy relative to raw Infutor data: in particular, it reduces the deviation from ground truth ACS county-to-county migration estimates by 90%. We document systematic demographic biases in the Infutor data, which overcounts rural, older, white, and home-owning populations, and show that **MIGRATE** almost entirely eliminates these biases. To illustrate the benefits of granular migration data, we provide a case study using our estimates to study migration in response to California wildfires, showing that **MIGRATE** reveals dramatic increases in out-migration which county-level data obscures. To provide a foundation for more precise migration research in the social, environmental, and health sciences, we release **MIGRATE** for other researchers at migrate.tech.cornell.edu.

2 Creating **MIGRATE**

Here we provide a high-level summary of our method for inferring fine-grained migration matrices by harmonizing Census and Infutor data. In the Appendix, we provide full details of processing the Infutor dataset (Appendix A), processing Census data (Appendix B), and harmonizing the two data sources (Appendix C).

Preprocessing the raw Infutor dataset

We first preprocess the raw Infutor data into yearly migration matrices. The raw Infutor data consists of sequences of addresses for individual people. We use this information to compute the number of people moving between each pair of geographic areas. In particular, we estimate the matrices $E^{(t)}$, where entries $E_{ij}^{(t)}$ represent the number of people who reside in CBG j some time during year t and resided in CBG i a year prior. We provide descriptive statistics for the raw Infutor data and the processed migration matrices for the 2010-2019 time period in Table 1 and additional descriptive statistics in Appendix Table A1.

Preprocessing Infutor requires mapping addresses to geographic areas. When the raw Infutor data contains a precise street address (90.40% of all addresses in the dataset), we map each address to a unique 2010 CBG with a state-of-the-art geocoder [22, 23]. We obtain matches for 92.18% of these addresses and confirm by hand inspection of 200 addresses that this yields highly accurate results. The remaining addresses are incomplete or imprecise (e.g., contain only ZIP codes); we probabilistically map these addresses to multiple CBGs, with the weight of each CBG proportional to the population in the CBG intersecting the ZIP code. We are able to map 99.21% of all addresses in Infutor to CBGs. We fully describe the extensive additional preprocessing steps for the raw Infutor data — including

Individuals with active records (any time in 2010-2019)	374,217,253
Individuals with active records in a given year (average across 2010-2019)	231,270,602
US population in 2010	309,327,143
US population in 2019	328,329,953
Address records per active individual (mean)	2.67
Address records per active individual (median)	2

Table 1: Summary statistics for raw Infutor data and Census data during the period of interest (2010-2019). We define “individuals with active records” as those whose [earliest Infutor date observed, latest Infutor date observed] interval intersects a given time period. Comparing the average yearly number of active individuals in the Infutor data to the Census population shows that Infutor under-counts the population. (Table A1 provides the number of active individuals in each year from 2010-2019). Active individuals have on average between two and three addresses, translating to one or two moves during the decade.

accounting for uncertainty in move date, choosing between geocoders, and prioritizing addresses for individuals with conflicting histories — in Appendix A.

Harmonizing the Infutor and Census datasets

Having produced the raw Infutor yearly migration matrices $E^{(t)}$, we next reconcile them with more reliable but less granular Census data by rescaling selected entries of $E^{(t)}$. For example, to reconcile $E^{(t)}$ with Census county populations at time t , we multiply the rows corresponding to each county by a scaling factor to match the Census population in that county. We rescale to different Census datasets in sequence, rather than simultaneously, because the datasets are not totally consistent with each other.

Specifically, we first rescale the entries of $E^{(t)}$ to match CBG populations; then the 1-year counts of movers and non-movers by state; then the 1-year state-to-state flows; and finally the 1-year county populations. The motivation for this ordering is that the 1-year county populations are more precisely estimated than the other datasets, and we thus prioritize matching to them: while CBG populations and state flows are estimated by the American Community Survey (ACS) and often contain large sampling errors, county populations are estimated by the Population Estimates Program (PEP) using more precise large-scale administrative datasets. We verify that incorporating each of these datasets improves our performance on the validations discussed below, and that the performance is not overly sensitive to the order in which we match to the datasets (see Appendix D.2). To match each matrix

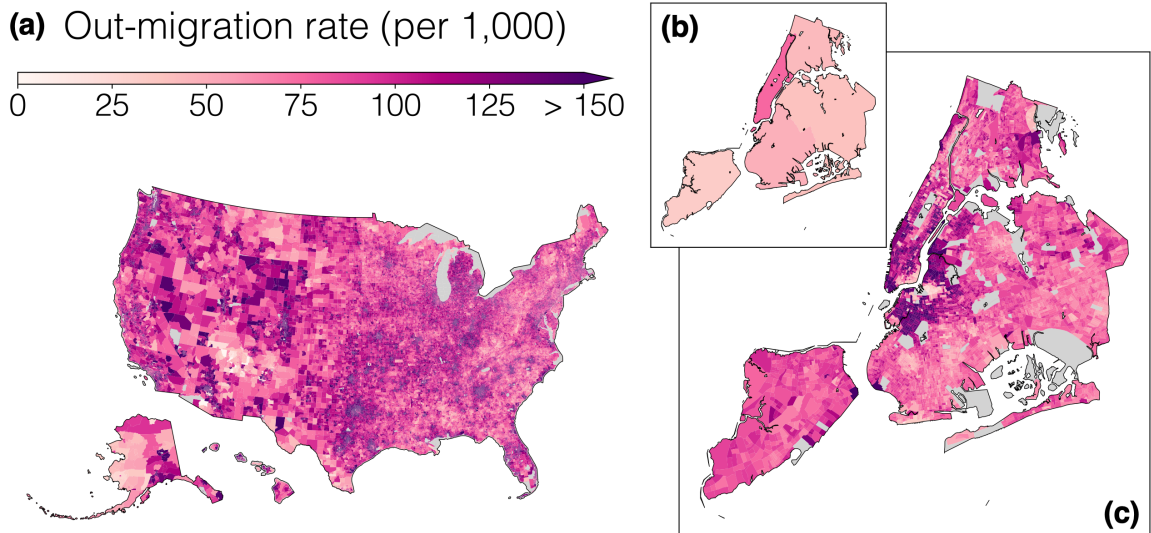


Fig. 1: MIGRATE estimates. We estimate annual migration flows between all pairs of Census block groups (CBGs) from 2010-2019. (a) Average MIGRATE estimates of out-migration rates across the entire United States. (b-c) MIGRATE estimates of out-migration rates within New York City. MIGRATE estimates reveal granular spatial patterns invisible in publicly available county-to-county data (inset plot (b)). Out-migration rates for CBGs with fewer than 100 people are omitted.

$E^{(t)}$ to annual county populations, we apply an IPF-based algorithm [21, 24]: we scale blocks of rows and columns to agree with the annual county populations in years $t - 1$ and t , respectively, alternating between scaling rows and scaling columns until the procedure converges (Appendix C.4). The resulting migration matrices constitute our MIGRATE estimates. Appendix C provides additional methodological details on these scalings.

Naive implementations of our harmonization algorithm impose prohibitive computation times due to the size of the matrices involved. We rely on the sparsity of the problem to dramatically reduce both memory and time requirements, allowing our procedure to converge within 2 hours using 16G of memory and 8 cores. Our general approach — i.e., rescaling submatrices to match Census constraints — can straightforwardly be adapted to accommodate other sources of Census data.

Figure 1 depicts the MIGRATE estimates. Figure 1a plots the average out-migration rates for all CBGs in the United States in the 2010-19 period, highlighting the spatial granularity of the estimates. This granularity often reveals important patterns which are invisible at the county-county level, as we illustrate by zooming in on New York City and comparing the county-level rates obtained from ACS flows (Figure 1b) to the CBG-level out-migration rates inferred by MIGRATE (Figure 1c). In Appendix E, we include an additional analysis showing how the socioeconomic stratification of movers’ destinations changes depending on whether we look at county-level estimates or MIGRATE estimates: residents from lower-income CBGs in higher-income counties tend to move to other lower-income CBGs, but this trend is obscured at the county level.

3 Validating MIGRATE

We conduct extensive validations of the MIGRATE estimates. We first show that MIGRATE estimates are highly concordant with Census datasets and improve agreement relative to raw Infutor data (Figure 2). We then investigate demographic biases in the raw Infutor estimates and show that MIGRATE reduces them (Figure 3).

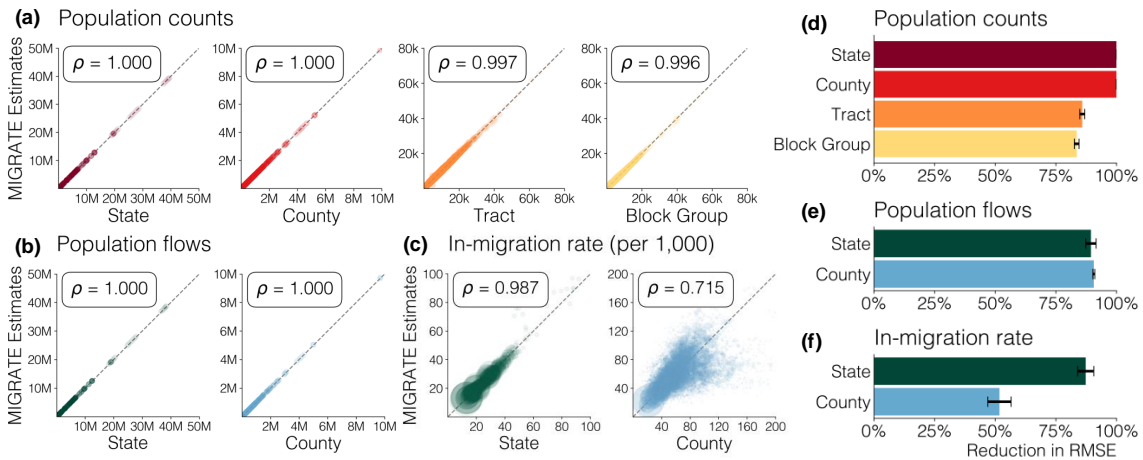


Fig. 2: Validating the MIGRATE estimates. MIGRATE estimates are highly correlated with (a) Census populations at the state, county, tract, and block group level, (b) Census flows between each pair of states and each pair of counties, and (c) state and county in-migration rates (i.e., the number of people moving into an area as a fraction of the area’s population). For in-migration rates, correlations are weighted by state or county population, and points are sized by population. (d - f) MIGRATE estimates increase agreement with Census datasets relative to raw Infutor data. We compute RMSE between (1) MIGRATE estimates and Census data and (2) Infutor data and Census data, and report the reduction in RMSE from using MIGRATE estimates. Bars show the mean reduction in RMSE across all years; error bars plot standard deviation across years. For the in-migration rates, RMSE is weighted by area population.

MIGRATE estimates are highly correlated with ground-truth Census data

MIGRATE estimates are well-correlated with all available Census measures (Figure 2a-b). We first assess correlations with Census datasets incorporated in our harmonization procedure, to confirm it indeed helps reconcile MIGRATE with Census data. We would expect these correlations to be high but not uniformly perfect, because the Census datasets are not totally consistent with each other. By design, MIGRATE estimates perfectly match state and county populations (because the last step in our procedure is to match to county populations). MIGRATE estimates also achieve Pearson correlation $\rho = 0.997$ with 5-year Census tract populations, and $\rho = 0.996$ with 5-year CBG populations¹. MIGRATE estimates are also highly correlated with state-to-state flows ($\rho = 1$); this high correlation is driven in part by variation in state populations, as well as by the fact that most people do not move. Hence, we also compute correlation with state in-migration rates ($\rho = 0.987$), which is not subject to either of these effects; in Appendix D.1, we report additional validations using diagonal and off-diagonal flow entries, as well as raw in-migration, which are also highly correlated with our estimates.

Importantly, we further verify that our estimation procedure yields highly correlated estimates even with datasets which are *not* used in our estimation procedure. This constitutes a validation on *held-out data*, a standard check for statistical estimation methods [25]. Specifically, we compare our MIGRATE estimates to ACS 5-year county-to-county flows, which are not incorporated in our estimation, and find they are highly correlated with our estimates ($\rho = 1$). This high correlation is driven in part by the fact that most people do not move; hence, in Appendix D.1, we compute correlations separately for county movers and county non-movers (all above $\rho = 0.95$), as well as raw in-migration ($\rho = 0.992$). Another contributor to the high correlation in county-county flows is variation in county size, so we separately compute correlations with county in-migration rates (i.e., the number of people moving into an area as a fraction of the area’s population) which normalize for county size. Correlations remain high (population-weighted $\rho = 0.715$).

As a further held-out validation, we verify that our estimation procedure yields highly correlated estimates with each Census data source even when we remove it from the datasets used for estimation: for example, we remove CBG-level Census populations from our estimation datasets, and verify that our resulting estimates remain highly correlated with CBG-level data ($\rho = 0.888$ with Census Tract populations and $\rho = 0.856$ with Census block group populations). See Appendix D.2 for full results.

Overall, these validations demonstrate that MIGRATE estimates are highly correlated with external ground-truth Census data. This is not merely because of variation in state or county size (since it remains true when examining in-migration rates, which normalize for state or county size, as well as when looking at the tract and CBG level). Nor is it due merely to the fact that most people do not move (since it remains true when examining correlations for movers specifically). Finally, it is not merely a consequence of overfitting to Census data, because it remains true on held-out datasets which are not used in our estimation procedure.

MIGRATE estimates reduce error relative to raw Infutor data

We show that MIGRATE estimates also increase agreement with Census datasets compared to using the Infutor data. We note that Infutor systematically undercounts the population (Table 1); to compare to Infutor as generously as possible, and in particular to ensure that MIGRATE does not reduce error due to trivial rescalings, we multiply each raw Infutor matrix $E^{(t)}$ by a scaling factor so it matches the national yearly Census population prior to conducting these comparisons. Figures 2c and 2d report the reduction in error that MIGRATE estimates achieve relative to Infutor data. We compute root mean squared error (RMSE) between (1) MIGRATE estimates and ground-truth Census data and (2) Infutor data and ground-truth Census data, and report the reduction in RMSE from using MIGRATE estimates. We show average reduction in RMSE across all data releases between 2010 and 2019; error bars represent standard deviation across these releases.

MIGRATE estimates eliminate error in state and county populations because they are constructed to match county-level estimates. Relative to raw Infutor data, MIGRATE estimates reduce error in Census tract populations by an average of 85.9% and error in CBG populations by 83.6%. MIGRATE estimates reduce error in state-to-state flows by 89.5% and error in state in-migration rates by 83.3%. We provide error reductions for additional metrics (movers, non-movers, and in-migration) in Appendix D.1.

¹To compare our one-year MIGRATE estimates to five-year ACS estimates, we average our estimates across the same periods for consistency with the ACS data. We only use ACS data products whose period completely overlaps with the 2010-2019 MIGRATE range.

We again confirm that we still see these reductions in error on held-out data which is not used in our estimation procedure. Specifically, MIGRATE reduces error in county-to-county flows by 90.6% and error in county in-migration rates by 49.9%. Neither of these datasets was used in producing MIGRATE estimates. We also repeat the validation above where we successively remove types of data (e.g., CBG-level populations) from our estimation procedure, and verify that our estimation procedure still reduces error in reproducing those held-out data types (Appendix D.2). Collectively, these validations demonstrate that MIGRATE estimates increase agreement with Census datasets, including held-out datasets, compared to raw Infutor data.

MIGRATE estimates reduce demographic biases present in raw Infutor data

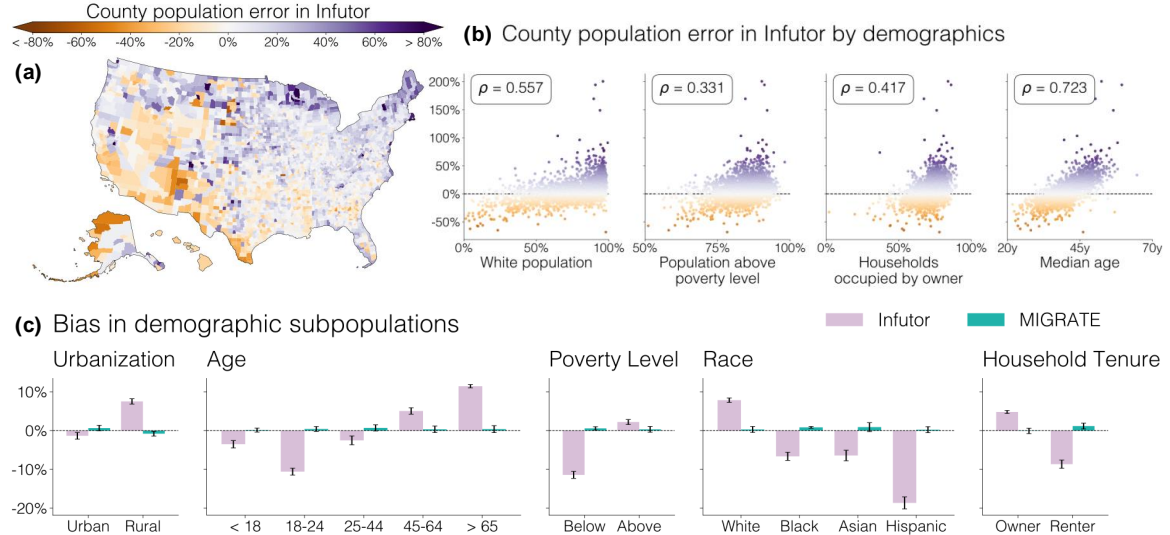


Fig. 3: Assessment of demographic bias in the raw Infutor data and the MIGRATE estimates. Infutor data displays biases which MIGRATE estimates greatly reduce. (a) Average errors in county populations in Infutor data relative to Census data; orange denotes counties where Infutor underrepresents the population, and purple denotes counties where Infutor overrepresents it. MIGRATE estimates remove all county-level errors by construction. (b) Spearman correlation between county demographics (x-axis) and error in Infutor estimates (y-axis). Infutor’s error is correlated with racial, socioeconomic, and other demographic characteristics. (c) Comparison of demographic bias in Infutor (purple) and MIGRATE (green). Bars compare demographic subpopulations estimated from Infutor or MIGRATE to ground-truth Census data. MIGRATE greatly reduces biases for all demographic subgroups.

The Infutor data displays geographic and demographic biases (Figure 3). Specifically, it overrepresents populations in the counties in the northeastern United States while underrepresenting populations in the southwest (Figure 3a).² Errors plotted are averages of county population errors across all 10 years of data from 2010-2019. MIGRATE estimates remove all such county-level errors by construction.

Errors in the Infutor data also correlate with demographics (Figure 3b). Infutor data overrepresents White, home-owning, richer, and older populations: there is a positive Spearman correlation between the relative error in county population estimates and the population share of a county in each of these groups. These biases are consistent with biases found in previous research [20], as we discuss in detail in Appendix D.3, and could propagate into biases in downstream analyses of inequality and other topics.

MIGRATE estimates reduce biases in Infutor data. Figure 3c compares the demographic biases of the MIGRATE estimates to the biases of the Infutor data. To quantify bias, we compare (1) the ground-truth number of people within each group (from Census data) to (2) the number of people within each group estimated from Infutor or MIGRATE, which we compute as $\sum_i p_i \cdot n_i$, where i indexes

²For this analysis, as above, we multiply each Infutor matrix $E^{(t)}$ by a scaling factor so it matches the national yearly Census population to avoid deviations due to trivial rescalings.

CBGs, p_i is the proportion of people in a CBG within a given group (e.g., the proportion of Black residents) based on Census data, and n_i is the number of people in a CBG in Infutor or MIGRATE. This quantifies how much Infutor and MIGRATE overcount or undercount a given demographic group, relative to ground-truth Census data. The raw Infutor data substantially overcounts rural, older, white, and home-owning populations, and undercounts younger, Black, Asian, Hispanic, renter, and below-the-poverty-line populations; the MIGRATE estimates almost entirely eliminate these biases. We present analyses for additional demographic groups, finding similar results, in Appendix D.4.

4 Case study: migration in response to California wildfires

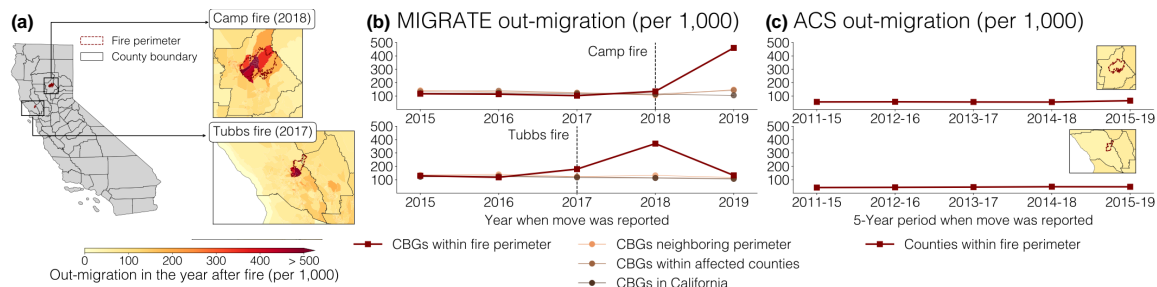


Fig. 4: Migration in response to California wildfires. (a) Out-migration following the Camp fire (2018; top) and Tubbs fire (2017; bottom). Red boundaries plot fire perimeters; black lines plot county boundaries; CBGs are colored by domestic out-migration rate in MIGRATE. Out-migration rates exceed 50% in many CBGs within the fire perimeters. (b) Out-migration rates in different groups of CBGs over time according to MIGRATE estimates. Out-migration rates in the year after the fire are higher in CBGs within the fire perimeter (red line) than in groups of CBGs outside the fire perimeter (other lines), including those neighboring the fire perimeter, those in affected counties, or those within California. (c) Out-migration rates in ACS 5-year county-to-county data remain relatively constant over time.

We demonstrate the value of the MIGRATE estimates by using them to study migration in response to wildfires in California. Natural disasters, including wildfires, are known drivers of human mobility [3, 26]. There were over 3,000 fire events in California from 2010-2019, which cumulatively affected nearly 27,504 square kilometers — approximately 6.5% of the California land area. In many US states, including California, wildfire risk increased from 2010-2019 [27], and is expected to further increase due to climate change [28]. Researchers rely on a variety of data sources, such as administrative records and building codes, to study vacancy and movement following these disasters [29].

Post-wildfire migration estimates can inform disaster response and long-term planning in multiple ways. First, migration data is crucial for policymaking in the aftermath of a wildfire. It helps guide the allocation of housing, public health, and other resources to support displaced residents while minimizing strain on housing markets in receiving areas [26, 30–32]. Data on out-migration rates from affected areas can also inform decisions about whether and how to rebuild in fire-prone regions [33, 34]. Second, high-resolution migration data is important for future wildfire planning. As populations relocate in response to shifting wildfire risks, migration patterns can refine policymakers’ estimates of future risk and guide the regulation of housing and insurance markets [35–39]. While some households may move to reduce their exposure, others may become “trapped” in high-risk areas due to financial, social, or logistical barriers [40–42]. Identifying these communities through high-resolution migration data can help ensure that government support reaches those who need it most [34, 43].

We use high-resolution fire perimeter data from the California Department of Forestry and Fire Protection [44]. Fire perimeters are typically much smaller than county boundaries, suggesting that analyzing fire impacts may require the granularity of the MIGRATE estimates as opposed to the relatively coarse county-to-county flows. We analyze the two most destructive fires in California from 2010-2019 (as quantified by the number of structures lost to the fire): the Tubbs Fire in October 2017, and the Camp Fire in November 2018 (Figure 4). The Tubbs Fire occurred in Napa County and Sonoma County and destroyed at least 5,636 residential or commercial structures [45]. The Camp

Fire, about a year later, destroyed over 18,804 structures and damaged nearly 1,000 more in the Northern California county of Butte [46]³.

MIGRATE estimates reveal dramatic levels of out-migration for CBGs which lie within the fire perimeters (Figure 4a) in the year following the fires, often exceeding 50%.⁴ In contrast, CBGs which do not lie within the fire perimeters experience much lower out-migration rates. We systematically quantify these differences in Figure 4b, which compares CBGs within the fire perimeter to three sets of less-affected CBGs outside the perimeter: other CBGs neighboring the perimeter; other CBGs within the affected counties; and others within California as a whole. The out-migration rate in the year following the Camp Fire for CBGs within the fire perimeter is 46%, at least $3.1\times$ that of less-affected CBG groups; the out-migration rate in the year following the Tubbs Fire for CBGs within the perimeter is 37%, at least $2.8\times$ that of less-affected CBG groups. Our estimates of out-migration following the Camp Fire are similar to those in prior work [26].

In contrast, publicly available county-level migration data obscure these dramatic out-migrations; Figure 4c shows that rates of out-migration in affected counties remain essentially flat. This happens because the county-level data is both too spatially and too temporally coarse: the county boundaries include many CBGs unaffected by the fire, and the estimates are aggregated over 5 years. Further, many people displaced by the Camp and Tubbs Fires moved to other CBGs within the affected counties (and thus would not be counted as movers in the county-level data): 77% of movers from CBGs within the Tubbs fire perimeter and 54% of movers from CBGs within the Butte Fire perimeter remained within the affected counties.

ACS 5-year CBG population estimates similarly obscure the dramatic levels of out-migration due to their lack of temporal granularity. In the year following the fires, MIGRATE estimates reveal population declines 260% larger in magnitude for the Tubbs fire and 40% larger in magnitude for the Camp fire than those visible at the 5-year ACS level. (For this analysis, we compare to the relative change in the ACS 5-year dataset released the year following the fire from the ACS 5-year dataset the year before: for example, for the 2018 Camp Fire, we compare the 2015-2019 ACS estimates to the 2014-2018 ACS estimates.) The ACS 5-year population estimates, unlike MIGRATE estimates, also provide no insight into the destinations of out-movers.

Collectively, these analyses showcase how MIGRATE estimates reveal substantial, policy-relevant responses to wildfires which traditional data sources conceal. Indeed, the MIGRATE estimates enable further analyses beyond those conducted here: for example, they can illuminate inequality in responses to wildfires by connecting out-migration patterns with CBG-level demographics.

5 Discussion

We produce MIGRATE, a dataset of spatially and temporally fine-grained migration matrices capturing annual flows between pairs of CBGs from 2010-2019. Our estimates are approximately 4,600 times more spatially granular than publicly available county-to-county 5-year migration data, and 18 million times more spatially granular than state-to-state 1-year migration data. We produce these estimates by developing an IPF-based algorithm to harmonize granular but biased proprietary migration data with more reliable but less granular Census datasets.

We show that MIGRATE estimates correlate highly with external Census ground-truth datasets and reduce error and demographic bias relative to the raw proprietary data. We discuss the measures taken to protect the privacy of all individuals in the dataset in Appendix F. Our estimates are available at migrate.tech.cornell.edu.

While we validate MIGRATE estimates comprehensively against external data sources, practitioners making use of the data should be mindful of two limitations. First, while we use multiple ground-truth Census data sources to reduce the biases we document in the raw Infutor data, uncorrected biases likely remain. For example, while we correct biases in CBG populations, we cannot correct sub-CBG-level population biases, or biases in CBG-CBG flows. Second, while we show that MIGRATE estimates are highly correlated with external Census datasets (including held-out datasets which are not included in producing our estimates), these validations have imperfections. As we further describe in Appendix B.2, Census datasets themselves have biases; can possess significant margins of error, particularly at fine spatial scales; and are not perfectly consistent with each other.

³The Camp Fire remains the most destructive wildfire in California as of early 2025; the Tubbs Fire has only been surpassed by the January 2025 Eaton and Palisades fires [47].

⁴The fact that the out-migration rate is not 100% is likely due to a number of factors, including the often-preferred option of rebuilding and returning [37, 38]. Looking at administrative address data from mail delivery after Camp Fire, for example, researchers found a much more significant uptick in short-term vacancy than in long-term vacancy [29].

Another challenge in validation is the lack of a ground-truth CBG-CBG migration matrix against which to validate; publicly available Census datasets do not afford this level of granularity, and non-Census data sources (e.g., voter files) have significant biases and measure substantively different populations than the one we seek to model [48, 49]. Overall, MIGRATE should be viewed as a new data source which like all data possesses limitations but nonetheless represents a significant improvement on widely used publicly available data sources (due to its granularity) or proprietary data sources (due to reductions in error and bias).

We hope these improvements will facilitate a wide range of further migration-related analyses. As our wildfire case study illustrates, MIGRATE reveals patterns which remain invisible in publicly available migration data. The fine spatial scale of the data also enables analyses of *inequality* in migration, by linking migration patterns to CBG-level demographics. Our work also highlights methodological directions for improving estimation of fine-grained migration patterns, including providing principled margins of error on estimates and incorporating additional data sets to further improve estimation and validation. More broadly, we hope MIGRATE will facilitate more precise study of many migration-related phenomena across the social, health, and environmental sciences.

Appendix A Processing Infutor Data

Infutor provides data in tabular form. Each row in the data provides data for one individual, which includes a list of known addresses, along with the date when the individual is first observed at the address (which we refer to the *effective date* below), and the first and last date that the individual is observed in the data (which we refer to as the *listed start date* and the *listed end date*, respectively).⁵ Dates are listed as month and year. For example, the data for one individual might consist of two addresses: “1 Main Street, Everytown, USA, 10000 (January 2010); 2 Cornelia Street, New York, New York, USA (December 2017)” followed by an initial date of January 2008 and an end date of December 2017. We describe the steps taken to (1) identify and clean Infutor data records within the scope of MIGRATE, (2) process the Infutor data into matrices documenting yearly flows between address pairs, and (3) map these address-level matrices to the CBG-level matrices $E^{(t)}$ mentioned in the main text. Table A1 summarizes the raw and processed data.

A.1 Cleaning address histories

We first create a sequence of monthly addresses for each individual in Infutor: i.e., the address at which they are living each month. This requires us to resolve any inconsistencies in the dates provided by Infutor and model uncertainty in address histories.

We define the *interval of activity* during which each individual is active (observed) in the Infutor data. For each individual, we define their *reconciled start date* as the minimum of their first effective date, and their listed start date. We similarly define their *reconciled end date* as the maximum of their last effective date, and their listed end date. (For example, if the effective date list for an individual was [January 2013, January 2016], their listed start date was January 2014, and their listed end date was January 2017, their reconciled start date would be January 2013, and their reconciled end date would be January 2017.) Finally, we define their interval of activity as [reconciled start date – 1 year, reconciled end date + 1 year]. We use 1-year padding to reflect the annual granularity of the final dataset we produce and avoid discarding data in each yearly estimation process. This padding is also consistent with our treatment of deaths and emigrants, who will be recorded as non-movers in MIGRATE (and thus keep residence in the address they held during their last year alive in the United States).

Having defined each individual’s interval of activity, we define the address at which the individual is located for each month in that interval. This requires us to resolve inconsistencies in the address dates provided by Infutor, which we do as follows. We discard any addresses lacking an effective date, unless they are the only address for the individual—in such cases, we consider the reconciled start date also to be the effective date for that address. We discard any postal box addresses if there is a non-postal box address for an individual with an effective date within a year, since we assume that non-postal-box addresses are more reliable indicators of where someone lives. We then forward fill the remaining addresses so that each address spans span the period between its own effective date and the effective date of the next address. If the reconciled start date and reconciled end date for the individual differ from all the address effective dates, we fill these gaps with the first and last available addresses chronologically. If the individual has multiple addresses with the same effective date, we uniformly split the individual between the addresses by saying there was an equal probability of residence in any of them. At the end of this process, each individual is associated with a monthly probability distribution over addresses for each month in their interval of activity.

A.2 Processing address histories into annual address-address migration matrices

When then aggregate the monthly address histories for each individual to the annual level in a way which is consistent with the ACS interview process. We will ultimately reconcile the Infutor data with ACS geographic mobility data and thus want these datasets to be consistently processed. Our goal is to simulate the sampling process of ACS, in which any individual can be asked, throughout the year, where they lived one year ago (the specific wording of the ACS interview question is, “Where did this person live 1 year ago?”). To do so, we loop over the twelve months of the year and compute

⁵For a subset of individuals, Infutor also provides estimated demographic information (e.g., age, gender, and socioeconomic information). We do not incorporate this information in our analysis for two reasons: first, complete demographic data is only available for about half of all individuals; second, the reliability of estimated demographic information is concerning—as the data lacks documentation, we should not discard the possibility that demographic information has been imputed based on addresses—and contains known biases [20].

how the individual would answer this survey question if they were asked in each month, yielding flows between a pairs of addresses (where the individual currently resides, and where they resided a year prior).

We allow monthly flows to be probabilistic. For each pair of months in which the individual was certainly seen at single addresses, they would notify the ACS of that move (or stay) with probability one. However, if in one of the months there was uncertainty due to conflicting effective dates, the corresponding flow will also be uncertain; the individual might notify ACS they moved from *any* of the addresses they resided in the previous year during the month, or to *any* of the addresses they reside in the current year. We multiply probabilities of residence in each different address to obtain the probability of a flow; if the monthly address distribution remains constant in both years we assume permanence (i.e. the individual did not move) and report that individual possibly stayed in each listed address with its own residence probability. Accounting for this uncertainty yields a list with 3-tuples of addresses and a probability (ADDR1, ADDR2, $p_{1 \rightarrow 2}$) per month; weighting these tuples per month (according to the number of days in the month) yields an yearly distribution.

We then aggregate these yearly distributions over the entire Infutor data, we create a list of expected ACS responses for the full population. That is, if multiple people reported a flow between ADDR1 and ADDR2, we add all their individual probabilities and report a single combined flow between ADDR1 and ADDR2. This represents the expected number of individuals with that flow reported to ACS. Finally, we create an yearly set of matrices $A^{(t)}$ with dimension $N_{\text{ADDRESSES}} \times N_{\text{ADDRESSES}}$ (i.e. a square matrix on the number of unique Infutor addresses) where each entry $A_{ij}^{(t)}$ corresponds to the expected number of individuals moving between addresses i and j from year $t - 1$ to year t . These matrices will be further aggregated based on the location of each address.

A.3 Processing address-address migration matrices into CBG-CBG migration matrices

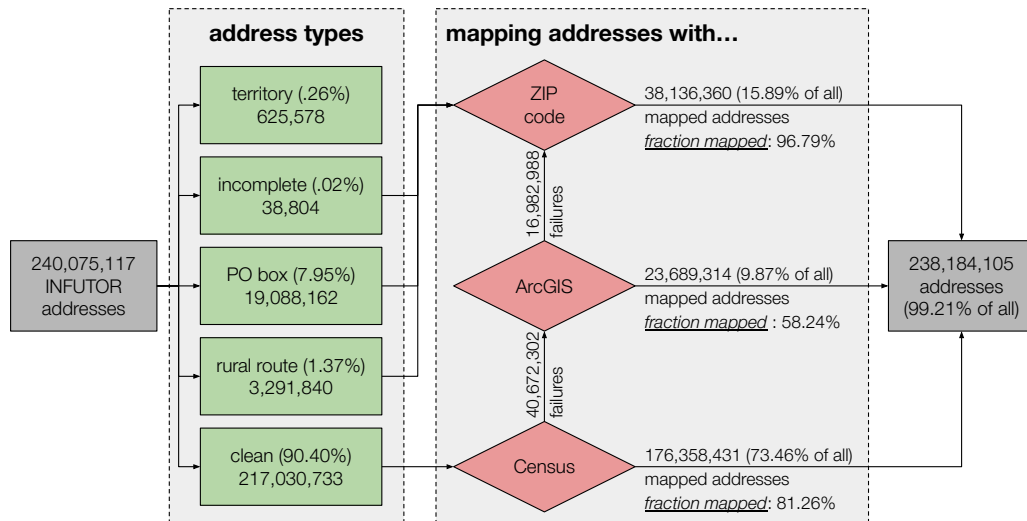


Fig. A1: Flowchart detailing the process of mapping addresses to CBGs. We start with all Infutor addresses and classify them into five address types. We remove addresses which lie within US territories but not US states (around .26% of the addresses). Incomplete addresses—those that do not have a precise street address line—as well as PO boxes and rural routes are mapped probabilistically to CBGs according to their ZIP code. The vast majority (90.4%) of addresses are clean, complete street addresses which are sent to the Census geocoder, which is able to map 81.26% of these addresses to a Census block group. If the Census geocoder fails to provide a match, we reattempt matching using ESRI’s ArcGIS geocoder; this achieves a lower match rate of 58.24%, in part because the sample it is applied to is more difficult to parse. In total, we are able to map 99.21% of all addresses in the original Infutor data: 83.33% to a precise latitude and longitude, and 15.89% to a ZIP code.

We transform the address-level migration matrices $A^{(t)}$ into CBG-level matrices $E^{(t)}$ by mapping each address either to a precise CBG where possible, or to a distribution over CBGs when only a ZIP code is available. We use the 2010 Census block group boundaries for all addresses to maintain geographic consistency. Figure A1 details this process.

Our address mapping pipeline is divided in two parts: mapping addresses via geocoding, and mapping addresses with a ZIP code-to-CBG crosswalk. We initially attempt to use one of two state-of-the-art geocoders to map addresses to latitudes and longitudes: the publicly-available Census Bureau geocoder [23] and ESRI’s ArcGIS geocoder [22]. We first attempt to geocode an address via the Census geocoder; if this algorithm does not find a match, we submit the address to ArcGIS. If neither algorithm finds a match, we map the address to Census Tracts intersecting its ZIP code, weighting probabilities based on the share of residential ZIP code addresses represented by the population of each Census Tract. Addresses representing rural routes and postal boxes are directly mapped via ZIP code, as well as incomplete addresses. We use the HUD ZIP-to-tract crosswalk, with the date closest available to the last seen date of an address to account for the fact that ZIP code definitions may vary and are not nested within Census geographies [50]. We then distribute the probability to each Census block group within the tracts, again weighting by their relative population shares. Success rates for each of these steps are high and detailed in Figure A1.

We use the results of this mapping process to create an auxiliary matrix \mathcal{G} of dimensions $N_{\text{ADDRESSES}} \times N_{\text{CBGS}}$. Each row of \mathcal{G} defines a probability distribution over Census block groups: an address i belongs to CBG j with probability \mathcal{G}_{ij} . If the address has been precisely mapped (i.e., geocoded via the Census or ArcGIS geocoders), the corresponding row of \mathcal{G} has a single entry equal to 1, with other entries 0. We use the matrix \mathcal{G} to compute the CBG-to-CBG matrix $E^{(t)}$ via the following equation:

$$E^{(t)} = \mathcal{G}^T \cdot \left[A^{(t)} - \text{diag} \left(A^{(t)} \right) \right] \cdot \mathcal{G} + \text{diag} \left[\mathcal{G}^T \cdot \text{diag} \left(A^{(t)} \right) \right] \quad (\text{A1})$$

where the $\text{diag}(\cdot)$ operator either converts a vector into a diagonal matrix or extracts the diagonal of a matrix as a vector. The first term in this equation maps *movers* to the appropriate entries of the migration matrix: for example, a precisely mapped move from CBG i to CBG j will increment $E_{ij}^{(t)}$ by 1, and a move from ZIP code a to ZIP code b will distribute mass (summing to 1) evenly across the sub-block whose rows lie within ZIP code a and columns lie within ZIP code b . The second term in this equation maps *stayers* to the appropriate diagonal entries of the migration matrix: for example, a precisely mapped stayer in CBG i will increment $E_{ii}^{(t)}$ by 1, and someone who stays within ZIP code a will distribute mass (summing to 1) evenly across the diagonal entries corresponding to CBGs within that ZIP code.

Table A1 reports a yearly breakdown of relevant Infutor data statistics throughout this pipeline. The number of individuals with active records in the data represents the number of individuals with an interval of activity containing each year at the start of the data processing; the number of CBG moves corresponds to the sum of off-diagonal entries of each matrix $E^{(t+1)}$ and measures the “effective size” of each year’s data: how many movers we actually account for at the beginning of the estimation procedure.

Year	(1) Active records	(2) US Population	(3) Effective Dates	(4) Processed CBG Moves
2010	269,228,776	309,327,143	48,225,002	15,180,982
2011	260,064,921	311,583,481	28,196,562	11,793,806
2012	259,451,204	313,877,662	32,009,822	12,544,199
2013	252,933,953	316,059,947	27,386,564	13,829,056
2014	256,453,630	318,386,329	37,386,684	13,071,070
2015	241,295,957	320,738,994	30,777,204	14,022,249
2016	242,298,262	323,071,755	38,085,337	13,605,804
2017	193,479,001	325,122,128	34,599,168	12,684,184
2018	177,629,604	326,838,199	33,183,982	13,505,890

Table A1: Yearly Breakdown of Data Summaries. Population and addresses accounted by the Infutor and Census datasets during the analysis period (2010-2019). **(1)** Individuals have active records in a given year if the year falls within their interval of activity in the dataset. The number of active individuals decreases in recent years, as Infutor records tend to appear when a move is reported. Comparison of these values to **(2)** the Census population shows that Infutor under-counts the population at every given year. **(3)** The number of effective dates per year is naturally reduced as we process the data into **(4)** CBG-to-CBG moves: an individual with two addresses will have at most one move, some addresses do not constitute residences, some individuals may have a single address in the year thus not move, etc.

Appendix B Processing Census Data

The U.S. Census Bureau runs multiple programs with the aim of counting and estimating demographic and socioeconomic population data. Each of these programs may release data at different spatiotemporal granularity and, even if geographies or timespans agree, the data might lack internal consistency. We use a series of steps to clean, select, and process Census datasets. We describe our procedures for reconciling Census geographies (§B.1), selecting which Census datasets to use as constraints (§B.2), and how we process the Census data to deal consistently with births, deaths, emigration, and immigration (§B.3).

B.1 Reconciling Census geographies

The United States is hierarchically divided into states, counties, Census tracts, Census block groups, and Census blocks, with each level subdividing its parent geography. Geographic boundaries are not necessarily consistent over time, and ensuring that population counts reflect the same geographic area across multiple years is essential when working with longitudinal data. For example, to produce multi-year estimates, the American Community Survey maps every reported address to the corresponding geography in the *current* year [51]. We use the 2010 Census boundaries for all addresses to maintain geographic consistency.

While the vast majority of geographies remain intact in the inter-decennial period (between Censuses, 2010-2020), there are some geography changes we must address. When geographies merge or split throughout the decade, we resolve the change by keeping only the coarser geographic boundary — i.e., the combined area which is the union of all finer-grained areas. With this approach, we can aggregate population statistics from the fine-grained areas into the coarse areas. There was one such county change in 2010-2019 affecting Bedford County in Virginia [52] and a few Census tract or Census block group changes documented yearly in the Census Bureau website (e.g. [53] for 2010 to 2011). When we aggregate ACS estimates that contain margins of error, we also aggregate margins of error in the L2 norm—as proposed by the ACS [54]. For our purposes, area renames are irrelevant. After these adjustments, MIGRATE considers a universe of 217,740 Census block groups grouped into 3,142 counties.

B.2 Selecting Census datasets

	2010	2011	2012	2013	2014	2015	2016	2017	2018	2019
CBG Populations	15.76	15.67	15.42	15.33	15.17	14.94	14.95	15.08	15.21	15.59
Tract Populations	6.41	6.24	6.03	5.95	5.79	5.60	5.50	5.54	5.56	5.66
County Flows	-	91.03	89.97	89.47	89.41	88.06	87.33	87.30	87.01	87.01
County Non-Movers	-	1.78	1.72	1.69	1.68	1.65	1.64	1.65	1.63	1.65
County In-Migration Rate	-	16.37	15.79	15.55	15.48	15.03	14.96	15.25	15.34	15.60
State Flows	-	47.61	45.47	45.14	44.23	45.33	45.76	46.31	45.62	47.31
State Non-Movers	-	0.41	0.39	0.39	0.38	0.40	0.40	0.38	0.37	0.39
State In-Migration Rate	-	4.95	4.68	4.79	4.65	4.70	4.76	4.72	4.85	5.02

Table B2: ACS Coefficients of Variation. Average coefficient of variation (in %) of the non-zero estimates in each dataset. CVs were computed as the ratio of the standard error (obtained by dividing the margin of error by 1.645) by the estimate [54]. We did not use flows released in 2010 (as they would report moves from 2009).

We rely primarily on three Census datasets: the ACS 5-year CBG populations; ACS 1-year state-to-state flows (from which we use raw flows as well as counts of non-movers and movers); and PEP 1-year county populations. PEP makes use of administrative records on births, deaths, and net migration to directly estimate county-level populations; the numbers reported contain the population estimate for July 1st of every year. ACS estimates, on the other hand, are a product of year-round surveying aggregated at the correspondent time scale, then released with associated margins of errors that define 90% confidence intervals [54]. Our dataset selection and methodology accounts for these different precision levels across the board.

We would like to avoid matching to datasets that were too noisily estimated. To decide which ACS datasets to use in our harmonization process, we examine their level of sampling error. We quantify the sampling error by the coefficient of variation (CV): the ratio of the standard deviation to

the estimate value. Table B2 reports the mean coefficient of variation in ACS estimates. In general, the number of non-movers has very low CVs (mean below 2% for counties and below 1% for states); population estimates have considerably lower CVs than flow estimates; state-to-state flows have relatively high CVs (mean around 45% every year), and county-to-county flows have extremely high CVs (mean almost 90%). We opt not to match to county-county flows due to the imprecision of raw flow estimates, although we do use them as a validation. In-migration rates have much tighter CVs than the corresponding flows (mean around 15% and 5% for counties and states, respectively), and we also use those as validations.

We perform a synthetic simulation study to verify that the datasets we do match to — state-to-state flows, and CBG population estimates — have sufficiently low sampling error to be reliably used. In particular, we resample each dataset using its reported margins of error, and compute correlations between the resampled data and the original data. To also assess mobility rates, we summarize state-to-state flows via the net migration rate. CBG populations and net state migration rates remain highly correlated with themselves after resampling (average Pearson correlation of $\rho = 0.976$ and $\rho = 0.766$, respectively).

Based on these analyses, we harmonize the entries of each yearly matrix $E^{(t)}$ with the following data: (1) CBG populations (both from 2010 Census and 5-year ACS); (2) ACS 1-year counts of movers and non-movers by state; (3) ACS 1-year state-to-state flows; and (4) PEP 1-year county populations.

B.3 Accounting for natural population increase and international migration

Using Census datasets to constrain MIGRATE estimates requires ensuring that the Census datasets reflect the same population accounted for in the Infutor matrix $E^{(t)}$. Each entry $E_{ij}^{(t)}$ represents the expected number of people alive with a residence in area i at year $t - 1$ and with a residence in area j at year t , and diagonal entries $E_{ii}^{(t)}$ also include individuals who resided in area i at year $t - 1$ but died or emigrated. We process the Census datasets so they reflect the same population, by accounting for changes in the populations at year t due to births, deaths, and international migration. Specifically, when using Census populations from year t to scale entries of $E^{(t)}$, we want to remove from each Census area population the natural increase in population (i.e., births minus deaths) and the net international migration (i.e., immigrants minus emigrants); when using Census flows from year $t - 1$ to year t , we want to add counts of deaths and emigrants back into the diagonal as non-movers. We adjust the Census constraints individually for every matrix $E^{(t)}$.

To do this adjustment, we make use of the PEP components of population change and ACS international immigration estimates. PEP releases estimates for the number of births, deaths, net international migration, and net domestic migration yearly at both a county and a state level [55]. To build yearly population estimates, PEP directly adds to the previous year’s estimates the natural increase, net international migration, and net domestic migration⁶. Whereas PEP estimates only report the net international migration, the ACS 1-year state-to-state flows also estimate the yearly number of immigrants per state (average CV around 12% across all years), which allows us to estimate the number of emigrants per state.

⁶PEP produces estimates that are geographically consistent: county-level estimates must aggregate precisely to state-level estimates, which must aggregate to nation-level estimates [55]. To achieve such precision, they also estimate small residuals at the county and state levels. We ignore these values.

Appendix C Harmonizing Infutor and Census Data

Having processed the Infutor and Census data, the final step in producing MIGRATE is to harmonize both data sources. Our harmonization process consists of scaling selected entries of the $E^{(t)}$ to match non-zero entries of Census datasets. We do not scale any entries to zero because the Census zeroes are noisily estimated, and subsequent multiplicative re-scalings cannot correct erroneous zero scalings. We detail below, in order, the scalings we conduct.

C.1 Harmonizing with CBG population data

First, we harmonize $E^{(t)}$ with CBG populations from the 5-year ACS estimates and the 2010 Census. We scale each row of each matrix $E^{(t)}$ such that the row sums — i.e., the CBG populations — are consistent with the constraints implied by the ACS 5-year CBG populations and the 2010 Census. For example, when we take the average sum of each row across the five matrices $\{E^{(2011)}, E^{(2012)}, E^{(2013)}, E^{(2014)}, E^{(2015)}\}$, this should be equivalent to the population for the corresponding CBG in the 2011-2015 ACS. Imposing these constraints corresponds to solving a linear system for each row using non-linear least squares (to impose the constraint that populations cannot be negative).

C.2 Harmonizing with yearly state non-movers data

Next, we harmonize $E^{(t)}$ with the counts of movers and non-movers by state from 1-year ACS data. To do this, we aggregate the off-diagonal entries of columns corresponding to each state and scale them to match the count of movers by state. We also aggregate the diagonal entries of columns corresponding to each state and scale them to match the count of non-movers by state. These scalings (which treat the population remaining within each CBG as equivalent to the population of non-movers) assume that very few people move to another location within the same CBG, an assumption substantiated by previous research.⁷

C.3 Harmonizing with yearly state-to-state flow data

We then harmonize $E^{(t)}$ with all state-to-state flows from 1-year ACS data. To do this, we aggregate the entries of the matrix $E^{(t)}$ according to the origin-destination state pair they belong to. For example, all flows from CBGs within Delaware to CBGs within Nevada are aggregated and scaled so that they sum to the total flow from Delaware to Nevada in ACS data. We do not scale to match zero flows.

C.4 Harmonizing with yearly county population data

We finally harmonize $E^{(t)}$ with county populations from 1-year PEP data. We choose to match $E^{(t)}$ to PEP populations last due to their superior reliability. In addition, PEP estimates are used internally by the Census Bureau as controls for many other datasets [57], and ensuring MIGRATE estimates agree with PEP can lead to better downstream agreement in other datasets.

To match to PEP county populations, we apply an IPF-based algorithm, alternating between two steps until convergence: (1) we aggregate the entries of $E^{(t)}$ by columns corresponding to each county and scale them to match the PEP county population at year t and (2) we aggregate the entries of $E^{(t)}$ by rows corresponding to each county and scale them to match the PEP county population at year $t - 1$. Our algorithm runs for 3,000 iterations, which we verify is sufficient for convergence. Specifically, at the end of 3,000 iterations, the total update to the matrix $E^{(t)}$ —that is, the L^1 distance between the resulting matrices in two subsequent iterations—falls to the order of 10^{-7} .

⁷Research has shown that median distance people moved in the US was about 10 to 15 miles in the 2010-19 period, which is far more than the average 2010 CBG radius (1.7 miles) and close to the 98-th percentile of radii [56].

Appendix D Validations

Here we provide additional details on MIGRATE validations. §D.1 provides additional validation metrics that complement Figure 2; §D.2 presents additional details on our held-out data validations; §D.3 provides details on related work documenting biases of Infutor, which is the subject of our Figure 3; and §D.4 presents additional socioeconomic and demographic dimensions on which we assessed biases.

D.1 Additional validation metrics

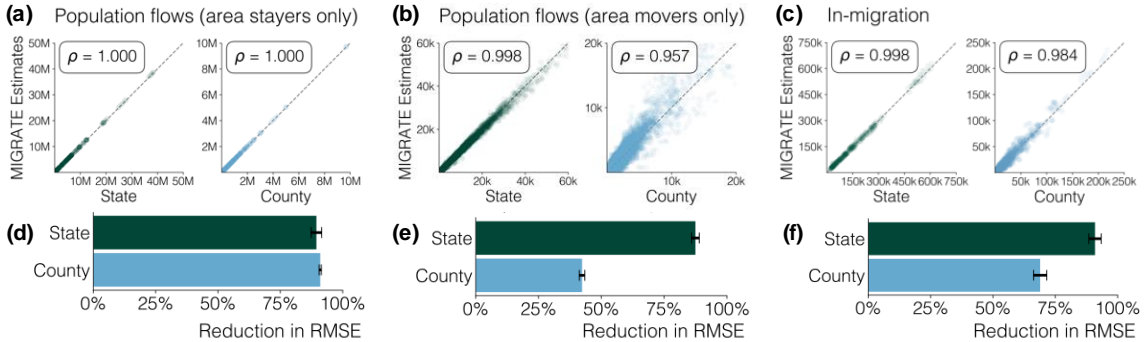


Fig. D2: Detailed flow validations of MIGRATE. To complement the findings shown in Figure 2, we present validations with respect to area stayers (i.e., the diagonal entries of the migration matrix), area movers (i.e. the off-diagonal entries of the migration matrix), and raw in-migration (i.e. the number of people arriving at an area). We show (a-c) Pearson correlations of estimates and selected ACS flows as well as (d-f) how much MIGRATE reduces RMSE compared to Infutor.

Figure D2 reports validation statistics for subsets of the migration matrices: in particular, area stayers (i.e., the diagonal entries of the migration matrix), area movers (i.e. the off-diagonal entries of the migration matrix), and raw in-migration (i.e. the number of people arriving at an area). We report these metrics at both the state and county level; state-to-state flows were used in the estimation procedure, county-to-county flows were held out. For all datasets, MIGRATE estimates are highly correlated with Census estimates (ρ above 0.957 in all cases) and reduce RMSE relative to the Infutor data.

D.2 Validating the estimation procedure using held-out data

We verify that our estimation procedure yields highly correlated estimates with each Census data source even when it is removed from the datasets used for estimation. For example, we remove CBG-level Census populations from our estimation datasets, and verify that our resulting estimates remain highly correlated with CBG-level data. Specifically, we conduct our full battery of validations on two additional sets of migration estimates: “CBG held-out”, which is estimated without the CBG-level population data (i.e. $E^{(t)}$ was not scaled to match ACS 5-year CBG populations); and “State held-out”, which is estimated without the state-level flow data (i.e. $E^{(t)}$ was not scaled to match ACS 1-year state-to-state flows nor state mobility rates). Table D3 reports values for the Pearson correlation across all estimates and ground-truth as well as relative error reduction from Infutor. Values for the original MIGRATE estimates, reported in Figure 2 and Figure D2, are reproduced for easy comparison.

The CBG held-out and State held-out estimates remain highly correlated with all Census datasets (ρ above 0.629); they also reduce RMSE relative to Infutor. Unsurprisingly, both the correlations and error reductions are smaller than those achieved by our full MIGRATE estimates, which make use of all sources of Census data. Together, these results illustrate both that (a) our estimation pipeline generalizes well to held-out data and that (b) all datasets used in the training help improve concordance with Census data, justifying their inclusion.

		MIGRATE	CBG Held-Out	State Held-Out
Population counts	State	1.000	1.000	1.000
	County	1.000	1.000	1.000
	Tract	0.997	0.888	0.998
	CBG	0.996	0.856	0.997
Population flows	State	1.000	1.000	1.000
	County	1.000	1.000	1.000
Population flows (area movers only)	State	0.998	0.998	0.895
	County	0.957	0.956	0.949
Population flows (area stayers only)	State	1.000	1.000	1.000
	County	1.000	1.000	1.000
In-migration	State	0.998	0.998	0.885
	County	0.984	0.983	0.963
In-migration rate	State	0.987	0.987	0.663
	County	0.715	0.705	0.629

(a) Pearson correlation between Census data and our estimates with CBG and state data held out. Pearson correlations with MIGRATE, which is estimated using all data sources, are presented for comparison.

		MIGRATE	CBG Held-Out	State Held-Out
Population counts	State	100.00	100.00	100.00
	County	100.00	100.00	100.00
	Tract	85.88	13.46	88.13
	CBG	83.60	9.08	85.09
Population flows	State	89.46	89.40	80.87
	County	90.65	90.70	75.24
Population flows (area movers only)	State	87.46	87.06	4.08
	County	42.34	41.30	4.65
Population flows (area stayers only)	State	89.46	89.40	81.03
	County	91.01	91.08	75.59
In-migration	State	90.93	91.11	7.22
	County	68.92	68.19	6.55
In-migration rate	State	87.30	87.33	4.89
	County	51.75	50.91	0.73

(b) Reductions in RMSE. We compute RMSE between (1) our estimates and Census data and (2) Infutor data and Census data, and report the reduction in RMSE from using our estimates. Positive values indicate improvements. Values are average reductions across all years with overlapping ground-truth data releases.

Table D3: Validation of estimates in held-out data settings. The full model validations are repeated for comparison. For in-migration rates, metrics are weighted by populations to account for disparate county and state sizes.

D.3 Related work documenting biases in the Infutor data

Many authors have assessed bias in the Infutor dataset, generally focusing on the data subsets or demographic characteristics most relevant to their own analyses. To our knowledge, the analysis we present in Figure 3 constitutes the first comprehensive documentation of biases in the Infutor dataset across (a) a long period of time and (b) the entire United States. We include here a non-exhaustive review of works with documentation of Infutor biases.

As we report in Table A1, Infutor undercounts the national US population. This is consistent with prior work; a similar finding is reported by Qian and Tan [19], Bernstein et al. [17], and Diamond et al. [15] among others. Phillips [16] additionally reports that, relative to 2010 ACS data, Infutor undercounts all state populations, but not by much, and out-of-state movers. A contrasting finding, reported by Diamond et al. [4], is that Infutor might overcount the population according to the 2000 Census in San Francisco. Such a finding might be driven by specific spatiotemporal idiosyncrasies of the San Francisco data in 2000, which is not included in the subset we analyze; however, the bulk of the literature, and all the literature which analyzes the same subset of the data we do, is consistent with our finding that Infutor undercounts the data. Diamond et al. [4] also suggest that Infutor might overcount populations due to lacking information about deaths; this is consistent with our finding that Infutor overcounts the older populations in Figure 3c.

In Figure 3, we also assess whether under- or over-represents demographic subpopulations. (Prior to conducting this assessment, we scale the Infutor population to match the overall population, so any discrepancies are not caused merely by overall undercounting.) Ramiller et al. [20] similarly

study representation biases of Infutor in King County, Washington, during the 2015-2019 5-year period. They find that Infutor undercounts the county population while overrepresenting White, older, home-owning, and high-income populations. Later, they regress population errors in tract-level demographics to find that Infutor records are overrepresented in areas with higher White and high-income populations among other characteristics. We confirm most of their findings in this limited spatiotemporal scale at national level. However, the authors use the NARC3 dataset—a subset of Infutor’s address records that contains detailed demographic information—and thus, beyond the spatiotemporal scope, our analyses might be substantially different.

D.4 Assessment of additional demographic biases

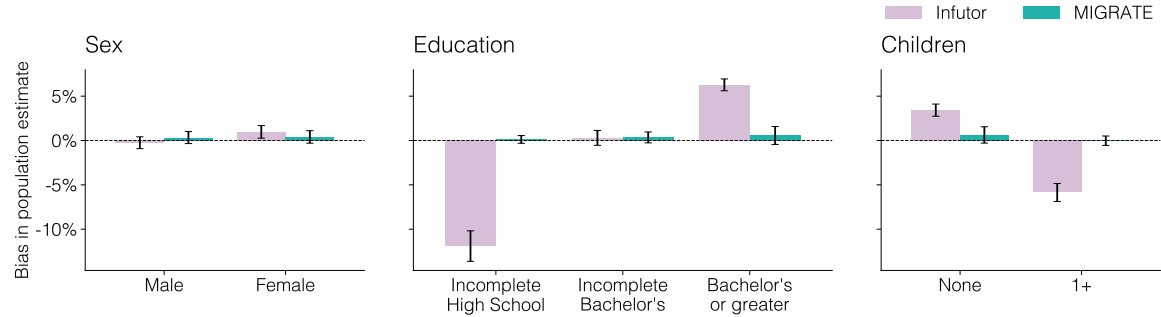


Fig. D3: Additional analysis of socioeconomic and demographic biases at CBG population level. Variables are taken from the 5-year ACS CBG estimates.

We documented biases in the Infutor dataset geographically (Figure 3a) and on the dimensions of urbanization, age, race, household tenure, and poverty (Figure 3c). Here, we provide additional analyses of demographic bias by sex, educational attainment, and number of children per household (Figure D3). We find that Infutor displays negligible bias on the basis of sex. However, Infutor underrepresents populations with less formal education while overrepresenting populations with more formal education. Populations living in households with no children are overrepresented while those in households with children are underrepresented. This finding is consistent with the Infutor data documentation, which describes a lack of records for people under the age of 18 (therefore, children will be undercounted). MIGRATE essentially eliminates biases along all these demographic dimensions.

Appendix E Case Study: Flows from New York City and Income

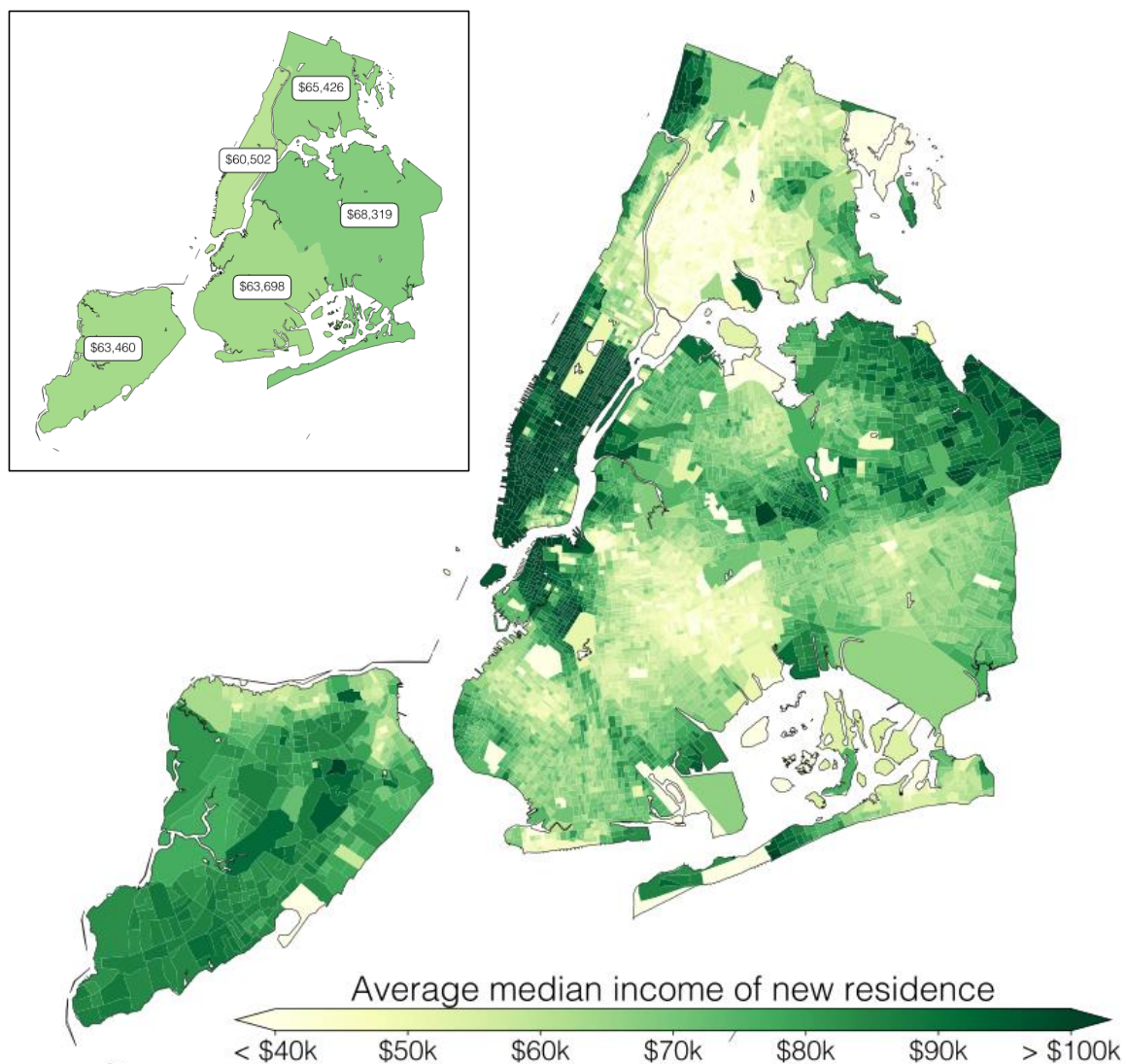


Fig. E4: Average median income of destination CBGs and counties for New York City out-movers in the 2010-19 period. The large map uses MIGRATE estimates and 5-year ACS CBG data. The inset map shows the corresponding distribution using only publicly available migration data from 5-year ACS county-to-county estimates.

We illustrate the value of MIGRATE estimates in an additional case study: contrasting MIGRATE with publicly available county-to-county migration data when analyzing migration stratified by a demographic or socioeconomic feature. Figure E4 plots the average median income of the CBG to which a person moves according to their previous CBG of residence. To compute this quantity for a given CBG i , we average the median income of all destination CBGs j for out-movers of CBG i weighted by the number of out-movers from i to j . We perform an analogous computation for the county plot in the inset.

Comparing these results to the data available at county level reveals striking within-county variation. For example, the median income of the county to which people from Manhattan moved was \$60,502—lower than that of the other four counties in New York City. MIGRATE reveals, however, that movers from some CBGs in Manhattan moved to areas with the highest median income among

all New York City CBGs — above \$100,000 — while movers from other Manhattan CBGs moved to areas with some of the lowest median incomes. Intra-county socioeconomic differences factor heavily in out-migration: Manhattan out-movers with the highest-income destinations tended to reside in the central and lower parts of the county (which tend to have higher incomes), whereas those with lower-income destinations came mostly from northern CBGs (which tend to have lower incomes). Similar within-county dynamics happen in the other four counties. Overall, this analysis illustrates the important demographic heterogeneity in migration which is concealed at the county level.

Appendix F Privacy Protections

In this section we detail the measures we took to preserve the privacy of individuals in the MIGRATE data release. Analysis of the Infutor dataset was determined to be not human subjects research by the Cornell Institutional Review Board (IRB #0145225).

First, in contrast to the original Infutor data, the data we release is aggregated: it contains only estimated migration between CBG-CBG pairs, and no information about individuals. This level of data aggregation is consistent with other data sources which have been made available to researchers. For example, mobility data often contains the aggregate counts of individuals moving from a given CBG to a given point of interest on a given day [58–62].

Second, the matrices we release are probabilistic and rescaled: in particular, the fact that a particular entry of the CBG-CBG migration matrix is non-zero does not guarantee that a given number of individuals moved between those CBGs (or indeed, that any did at all). This is because individuals are mapped probabilistically to CBGs (e.g., if we have only a ZIP code for an individual, they are mapped probabilistically to CBGs within that ZIP code) and the migration matrices are rescaled multiple times.

Third, we release the data only to researchers for non-profit use who agree to a data use agreement pledging not to re-identify individuals in the data, following manual review of their application and research project.

Finally, we compute the average number of destinations (unique CBGs) for out-movers from each CBG. The purpose of the analysis is to assess how difficult it would be to track a given individual if one knew they lived in a given CBG and then moved. Across CBGs and years, the mean number of destinations for outmovers is 272.2 (median 234). We redact from the public data release migration information for the very small proportion of CBGs (0.558%) for which 90% of out-movers travel to 10 or fewer CBGs. All analyses in the paper were conducted with the full data.

References

- [1] Hoffmann, R., Abel, G., Malpede, M., Muttarak, R., Percoco, M.: Drought and aridity influence internal migration worldwide. *Nature Climate Change* **14**(12), 1245–1253 (2024) <https://doi.org/10.1038/s41558-024-02165-1> . Publisher: Nature Publishing Group. Accessed 2025-01-24
- [2] Kaysen, R.: Open Houses in Los Angeles Take on an Eerie Feeling. *The New York Times* (2025). Chap. Real Estate. Accessed 2025-01-24
- [3] McConnell, K., Fussell, E., DeWaard, J., Whitaker, S., Curtis, K.J., St. Denis, L., Balch, J., Price, K.: Rare and highly destructive wildfires drive human migration in the U.S. *Nature Communications* **15**(1), 6631 (2024) <https://doi.org/10.1038/s41467-024-50630-4> . Publisher: Nature Publishing Group. Accessed 2025-01-24
- [4] Diamond, R., Guren, A., Tan, R.: The Effect of Foreclosures on Homeowners, Tenants, and Landlords. National Bureau of Economic Research (2020). <https://doi.org/10.3386/w27358> . <https://www.nber.org/papers/w27358> Accessed 2025-01-24
- [5] Wilkerson, I.: *The Warmth of Other Suns: The Epic Story of America’s Great Migration*. Knopf Doubleday Publishing Group, ??? (2010). Google-Books-ID: Y03WKII5m7QC
- [6] Niva, V., Horton, A., Virkki, V., Heino, M., Kosonen, M., Kallio, M., Kinnunen, P., Abel, G.J., Muttarak, R., Taka, M., Varis, O., Kummu, M.: World’s human migration patterns in 2000–2019 unveiled by high-resolution data. *Nature Human Behaviour* **7**(11), 2023–2037 (2023) <https://doi.org/10.1038/s41562-023-01689-4> . Publisher: Nature Publishing Group. Accessed 2025-01-24
- [7] DePillis, L.: For L.G.B.T.Q. People, Moving to Friendlier States Comes With a Cost. *The New York Times* (2024). Chap. Business. Accessed 2025-01-24
- [8] Ramani, A., Alcedo, J., Bloom, N.: How working from home reshapes cities. *Proceedings of the National Academy of Sciences* **121**(45), 2408930121 (2024) <https://doi.org/10.1073/pnas.2408930121> . Company: National Academy of Sciences Distributor: National Academy of Sciences Institution: National Academy of Sciences Label: National Academy of Sciences Publisher: Proceedings of the National Academy of Sciences. Accessed 2025-01-24
- [9] Kaysen, R., Singer, E.: Millions of Movers Reveal American Polarization in Action. *The New York Times* (2024). Chap. The Upshot. Accessed 2025-01-24
- [10] Shu, E.G., Porter, J.R., Hauer, M.E., Sandoval Olascoaga, S., Gourevitch, J., Wilson, B., Pope, M., Melecio-Vazquez, D., Kearns, E.: Integrating climate change induced flood risk into future population projections. *Nature Communications* **14**(1), 7870 (2023)
- [11] Craig, D.G.: America’s great climate migration has begun. here’s what you need to know. *Columbia Magazine* (2024). Accessed: 2024-12-05
- [12] Tedesco, M., Hultquist, C., Char, S.E., Constantinides, C., Galjanic, T., Sinha, A.D.: Socio-Economic, Physical, Housing, Eviction, and Risk dataset, version 2 (SEPPER 2.0), Preliminary Release (2021). <https://doi.org/10.7927/r6yw-xw73>
- [13] Kerns-D’Amore, K., McKenzie, B., Locklear, L.S.: Migration in the United States: 2006 to 2019. Technical Report ACS-53, American Community Survey (July 2023). <https://www.census.gov/content/dam/Census/library/publications/2023/acs/acs-53.pdf>
- [14] Infutor Data Solutions, LLC: Infutor Data Solutions - Batch Documentation (2019). <https://batchdocs.infutor.com/> Accessed 2025-03-20
- [15] Diamond, R., McQuade, T., Qian, F.: The Effects of Rent Control Expansion on Tenants, Landlords, and Inequality: Evidence from San Francisco. *American Economic Review* **109**(9), 3365–3394 (2019) <https://doi.org/10.1257/aer.20181289> . Accessed 2025-01-24

- [16] Phillips, D.C.: Measuring Housing Stability With Consumer Reference Data. *Demography* **57**(4), 1323–1344 (2020) <https://doi.org/10.1007/s13524-020-00893-5>
- [17] Bernstein, S., Diamond, R., Jiranaphawiboon, A., McQuade, T., Pousada, B.: The contribution of high-skilled immigrants to innovation in the united states. Technical report, National Bureau of Economic Research (2022)
- [18] Asquith, B., Mast, E., Reed, D.: Supply shock versus demand shock: The local effects of new housing in low-income areas. Available at SSRN 3507532 (2019)
- [19] Qian, F., Tan, R.: The effects of high-skilled firm entry on incumbent residents. Stanford Institute for Economic Policy Research (SIEPR) Working Paper, 21–039 (2021)
- [20] Ramiller, A., Song, T., Parker, M., Chapple, K.: Residential Mobility and Big Data: Assessing the Validity of Consumer Reference Datasets. *Cityscape* **26**(3), 227–240 (2024). Publisher: US Department of Housing and Urban Development. Accessed 2025-01-24
- [21] Deming, W.E., Stephan, F.F.: On a Least Squares Adjustment of a Sampled Frequency Table When the Expected Marginal Totals are Known. *The Annals of Mathematical Statistics* **11**(4), 427–444 (1940) <https://doi.org/10.1214/aoms/1177731829>
- [22] Hernangómez, D.: arcgeocoder: Geocoding with the ArcGIS REST API Service. (2024). <https://doi.org/10.32614/CRAN.package.arcgeocoder> . <https://dieghernan.github.io/arcgeocoder/>
- [23] U.S. Census Bureau: Census Geocoder User Guide. U.S. Government Publishing Office (2024). https://www2.census.gov/geo/pdfs/maps-data/data/Census_Geocoder_User_Guide.pdf
- [24] Chang, S., Koehler, F., Qu, Z., Leskovec, J., Ugander, J.: Inferring dynamic networks from marginals with iterative proportional fitting. *ICML* (2024)
- [25] Hastie, T., Tibshirani, R., Friedman, J.: *Elements of Statistical Learning: Data Mining, Inference, and Prediction*. 2nd Edition., 2nd edn. Springer, ??? (2009). <https://hastie.su.domains/ElemStatLearn/> Accessed 2025-03-14
- [26] McConnell, K., Whitaker, S., Fussell, E., DeWaard, J., Price, K., Curtis, K.: Effects of wildfire destruction on migration, consumer credit, and financial distress (2021)
- [27] Modaresi Rad, A., Abatzoglou, J.T., Kreitler, J., Alizadeh, M.R., AghaKouchak, A., Hudyma, N., Nauslar, N.J., Sadegh, M.: Human and infrastructure exposure to large wildfires in the United States. *Nature Sustainability* **6**(11), 1343–1351 (2023) <https://doi.org/10.1038/s41893-023-01163-z> . Publisher: Nature Publishing Group. Accessed 2025-02-27
- [28] Barbero, R., Abatzoglou, J.T., Larkin, N.K., Kolden, C.A., Stocks, B.: Climate change presents increased potential for very large fires in the contiguous united states. *International Journal of Wildland Fire* **24**(7), 892 (2015) <https://doi.org/10.1071/wf15083>
- [29] Din, A.: Graphic Detail: What Do Visualizations of Administrative Address Data Show About the Camp Fire. *Cityscape: A Journal of Policy Development and Research* (2022)
- [30] Rosenthal, A., Stover, E., Haar, R.J.: Health and social impacts of california wildfires and the deficiencies in current recovery resources: An exploratory qualitative study of systems-level issues. *PloS one* **16**(3), 0248617 (2021)
- [31] Hopfer, S., Jiao, A., Li, M., Vargas, A.L., Wu, J.: Repeat wildfire and smoke experiences shared by four communities in southern california: local impacts and community needs. *Environmental Research: Health* **2**(3), 035013 (2024)
- [32] Isaac, F., Toukhsati, S.R., Klein, B., Di Benedetto, M., Kennedy, G.A.: Differences in anxiety, insomnia, and trauma symptoms in wildfire survivors from australia, canada, and the united states of america. *International journal of environmental research and public health* **21**(1), 38

(2023)

- [33] McWethy, D.B., Schoennagel, T., Higuera, P.E., Krawchuk, M., Harvey, B.J., Metcalf, E.C., Schultz, C., Miller, C., Metcalf, A.L., Buma, B., *et al.*: Rethinking resilience to wildfire. *Nature Sustainability* **2**(9), 797–804 (2019)
- [34] Mach, K.J., Siders, A.: Reframing strategic, managed retreat for transformative climate adaptation. *Science* **372**(6548), 1294–1299 (2021)
- [35] Boomhower, J., Fowlie, M., Gellman, J., Plantinga, A.: How Are Insurance Markets Adapting to Climate Change? Risk Classification and Pricing in the Market for Homeowners Insurance. Technical Report w32625, National Bureau of Economic Research, Cambridge, MA (June 2024). <https://doi.org/10.3386/w32625> . <http://www.nber.org/papers/w32625.pdf> Accessed 2025-02-27
- [36] Patrick Baylis, J.B.: Mandated vs. voluntary adaptation to natural disasters: The case of u.s. wildfires. Technical Report w29621, National Bureau of Economic Research, Cambridge, MA (dec 2021). https://www.nber.org/system/files/working_papers/w29621/w29621.pdf Accessed 2025-02-27
- [37] Kramer, H.A., Butsic, V., Mockrin, M.H., Ramirez-Reyes, C., Alexandre, P.M., Radeloff, V.C.: Post-wildfire rebuilding and new development in California indicates minimal adaptation to fire risk. *Land Use Policy* **107**, 105502 (2021) <https://doi.org/10.1016/j.landusepol.2021.105502> . Accessed 2025-02-27
- [38] Alexandre, P.M., Mockrin, M.H., Stewart, S.I., Hammer, R.B., Radeloff, V.C.: Rebuilding and new housing development after wildfire. *International Journal of Wildland Fire* **24**(1), 138–149 (2014) <https://doi.org/10.1071/WF13197> . Publisher: CSIRO PUBLISHING. Accessed 2025-02-27
- [39] Lee, J., Costa, R., Baker, J.W.: Post-disaster housing recovery estimation: Data and lessons learned from the 2017 Tubbs and 2018 Camp Fires. *International Journal of Disaster Risk Reduction* **114**, 104912 (2024) <https://doi.org/10.1016/j.ijdrr.2024.104912> . Accessed 2025-02-27
- [40] Bohra-Mishra, P., Oppenheimer, M., Hsiang, S.M.: Nonlinear permanent migration response to climatic variations but minimal response to disasters. *Proceedings of the national academy of sciences* **111**(27), 9780–9785 (2014)
- [41] Cattaneo, C., Peri, G.: The migration response to increasing temperatures. *Journal of development economics* **122**, 127–146 (2016)
- [42] Benveniste, H., Huybers, P., Proctor, J.: Global climate migration is a story of who, not just how many. *Not Just How Many* (August 14, 2024) (2024)
- [43] Hino, M., Field, C.B., Mach, K.J.: Managed retreat as a response to natural hazard risk. *Nature climate change* **7**(5), 364–370 (2017)
- [44] California Department of Forestry and Fire Protection: Historical Fire Perimeters (2024). <https://www.fire.ca.gov/what-we-do/fire-resource-assessment-program/fire-perimeters> Accessed 2025-03-14
- [45] California Department of Forestry and Fire Protection: Tubbs Fire (Central LNU Complex) (2025). <https://www.fire.ca.gov/incidents/2017/10/8/tubbs-fire-central-lnu-complex> Accessed 2025-03-14
- [46] California Department of Forestry and Fire Protection: Camp Fire (2025). <https://www.fire.ca.gov/incidents/2018/11/8/camp-fire/> Accessed 2025-03-14
- [47] California Department of Forestry and Fire Protection: Top 20 Most Destructive California

- Wildfires (2025). <https://www.fire.ca.gov/our-impact/statistics> Accessed 2025-03-14
- [48] Fraga, B.L., Holbein, J.B., Skovron, C.: Using nationwide voter files to study the effects of election laws. Technical report, Working Paper, University of Virginia (2018)
- [49] Kim, S.-y.S., Fraga, B.: When Do Voter Files Accurately Measure Turnout? How Transitory Voter File Snapshots Impact Research and Representation. APSA Preprints (2022). <https://doi.org/10.33774/apsa-2022-qr0gd> . <https://preprints.apsanet.org/engage/apsa/article-details/6321ef75faf4a4ba6f1213ef> Accessed 2025-03-20
- [50] Wilson, R., Din, A.: Understanding and Enhancing the U.S. Department of Housing and Urban Development’s ZIP Code Crosswalk Files. *Cityscape* **20**(2), 277–294 (2018)
- [51] U.S. Census Bureau: 2024 ACS and PRCS Design and Methodology Version 4.0. U.S. Government Publishing Office (2024). https://www2.census.gov/programs-surveys/acs/methodology/design_and_methodology/2024/acs_design_methodology_report_2024.pdf
- [52] U.S. Census Bureau: Substantial Changes to Counties and County Equivalent Entities: 1970-Present. Section: Government (2021). <https://www.census.gov/programs-surveys/geography/technical-documentation/county-changes.html> Accessed 2025-03-19
- [53] U.S. Census Bureau: 2011 Geography Changes. Section: Government (2021). <https://www.census.gov/programs-surveys/acs/technical-documentation/table-and-geography-changes/2011/geography-changes.html> Accessed 2025-03-19
- [54] U.S. Census Bureau: Understanding and Using American Community Survey Data: What All Data Users Need to Know. U.S. Government Publishing Office (2020)
- [55] U.S. Census Bureau: Population and Housing Unit Estimates. Section: Government (2025). <https://www.census.gov/popest> Accessed 2025-03-15
- [56] Lautz, J.: Long-distance Movers: Why Did They Move and How? (2023). <https://www.nar.realtor/blogs/economists-outlook/long-distance-movers-why-did-they-move-and-how> Accessed 2025-03-20
- [57] U.S. Census Bureau: Population Controls for the 2021 ACS. Section: Government (2022). <https://www.census.gov/programs-surveys/acs/technical-documentation/user-notes/2022-10.html> Accessed 2025-03-15
- [58] Abbiasov, T., Heine, C., Sabouri, S., Salazar-Miranda, A., Santi, P., Glaeser, E., Ratti, C.: The 15-minute city quantified using human mobility data. *Nature Human Behaviour* **8**(3), 445–455 (2024)
- [59] Chang, S., Pierson, E., Koh, P.W., Gerardin, J., Redbird, B., Grusky, D., Leskovec, J.: Mobility network models of covid-19 explain inequities and inform reopening. *Nature* **589**(7840), 82–87 (2021)
- [60] Kostandova, N., Schluth, C., Arambepola, R., Atuhaire, F., Bérubé, S., Chin, T., Cleary, E., Cortes-Azuero, O., García-Carreras, B., Grantz, K.H., *et al.*: A systematic review of using population-level human mobility data to understand sars-cov-2 transmission. *Nature communications* **15**(1), 1–12 (2024)
- [61] Xu, F., Wang, Q., Moro, E., Chen, L., Salazar Miranda, A., González, M.C., Tizzoni, M., Song, C., Ratti, C., Bettencourt, L., *et al.*: Using human mobility data to quantify experienced urban inequalities. *Nature Human Behaviour*, 1–11 (2025)
- [62] Yabe, T., García Bulle Bueno, B., Frank, M.R., Pentland, A., Moro, E.: Behaviour-based dependency networks between places shape urban economic resilience. *Nature human behaviour*, 1–11 (2024)